Performance Enhancement of Primal-Dual Feedback-Based Optimization using Estimators

Niloufar Yousefi * **John W. Simpson-Porco** *

* *Department of Electrical and Computer Engineering, University of Toronto, 10 King's College Road, Toronto, ON, M5S 3G4, Canada*

Abstract: Feedback-based optimization (FBO) regulates a stable dynamical system to the solution of a constrained optimization problem under disturbances. However, closed-loop stability typically requires the controller to operate on a slower time scale than the plant, limiting closed-loop performance. An estimator-enhanced FBO (EE-FBO) removes this time-scale separation by incorporating plant model information via an extended-state observer. In this work, we extend EE-FBO for LTI systems to a class of primal-dual FBO controllers, and demonstrate its effectiveness via an application to fast power system frequency control using inverter-based resources.

Keywords: Linear Systems, Optimization : Theory and Algorithms, Feedback Control Systems

1. INTRODUCTION

The increasing complexity of engineered systems demands control frameworks that can reject disturbances, enforce constraints, and optimize performance (Farhat et al., 2025). Among existing approaches, feedback-based optimization (FBO) embeds simple optimization dynamics directly into the controller to steer a system toward an optimal equilibrium using real-time measurements and limited steady-state model information (Bianchin et al., 2022; Colombino et al., 2020). In this sense, FBO extends classical integral control from reference tracking to online optimization. A limitation of FBO is the need for time-scale separation between the plant and the optimization dynamics to guarantee stability, typically enforced through low controller gains. This requirement degrades transient performance and restricts applicability (Colombino et al., 2020).

Motivated by this limitation, we have developed a new FBO framework for LTI systems that removes the time-scale separation requirement in (Yousefi and Simpson-Porco, 2025) for projected gradient based optimization algorithms. The proposed method incorporates a model-based estimator that generates a real-time prediction of the plant's steady-state output. Injecting this estimate into the projected gradient FBO design ensures stability without sacrificing speed, thereby improving closed-loop performance and broadening applicability. Here we extend the EE-FBO approach to a broader class of FBO controllers, namely the proximal primal-dual controller proposed in (Colombino et al., 2020), which is capable of enforcing both input and output constraints.

2. FEEDBACK-BASED OPTIMIZATION

Consider the LTI system given by

$$
\begin{aligned}
\dot{x} &= Ax + Bu + Ew, \\
y_1 &= C_1 x, \\
y_2 &= C_2 x,
\end{aligned}
\tag{1}
$$

with state $x(t) \in \mathbb{R}^n$, control input $u(t) \in \mathbb{R}^m$, exogenous constant disturbance $w \in \mathbb{R}^q$ and measured output $y(t) = \mathrm{col}(y_1(t), y_2(t)) \in \mathbb{R}^p$ with $y_1(t) \in \mathbb{R}^{p_1}$ and $y_2(t) \in \mathbb{R}^{p_2}$. As a standard assumption in FBO (Hauswirth et al., 2024), we assume that the open-loop plant is asymptotically stable, i.e., A is Hurwitz. As a consequence, for any fixed input $u(t) = \bar{u}$, the state of (1) converges towards the unique equilibrium value $\bar{x} = -A^{-1}(B\bar{u} + Ew)$ and the equilibrium outputs are given by

$$
\bar{y}_1 = \Pi_{1u}\,\bar{u} + \Pi_{1w}\,w, \qquad \bar{y}_2 = \Pi_{2u}\,\bar{u} + \Pi_{2w}\,w,
$$

where

$$
\begin{aligned}
\Pi_{1u} &:= -C_1 A^{-1} B, & \Pi_{2u} &:= -C_2 A^{-1} B, \\
\Pi_{1w} &:= -C_1 A^{-1} E,' & \Pi_{2w} &:= -C_2 A^{-1} E.
\end{aligned}
$$

The goal is to design a controller which drives the output and control input of (1) towards the solution of the constrained steady-state optimization problem

$$
\begin{aligned}
\underset{\bar{u}, \bar{y}_1, \bar{y}_2}{\text{minimize}} \quad & f(\bar{u}) + h(\bar{y}_1) + g(\bar{y}_2) \\
\text{subject to} \quad & \bar{y}_1 = \Pi_{1u}\,\bar{u} + \Pi_{1w}\,w, \\
& \bar{y}_2 = \Pi_{2u}\,\bar{u} + \Pi_{2w}\,w.
\end{aligned}
\tag{2}
$$

where $f : \mathbb{R}^m \to \mathbb{R}$, $h : \mathbb{R}^{p_1} \to \mathbb{R}$, and $g : \mathbb{R}^{p_2} \to \mathbb{R} \cup \{\infty\}$ are convex costs placed on the equilibrium input and output values, respectively.

Assumption 2.1. The input cost f is continuously differentiable, μ_f-strongly convex, and its gradient ∇f is globally ℓ_f-Lipschitz continuous. The first output cost h is continuously differentiable, convex, and its gradient ∇h is globally ℓ_h-Lipschitz continuous. The second output cost g is convex, proper, and lower semicontinuous. The optimization problem (2) is feasible – and thus, by strong convexity of f possesses a unique optimal solution $u^\star$ – for all $w \in \mathbb{R}^q$.

The first equality constraint in (2) can be eliminated, yielding the equivalent problem

$$\underset{\bar{u}, \bar{y}_2}{\text{minimize}} \quad f(\bar{u}) + h(\Pi_{1u} \bar{u} + \Pi_{1w} w) + g(\bar{y}_2) \tag{3}$$
$$\text{subject to} \quad \bar{y}_2 = \Pi_{2u} \bar{u} + \Pi_{2w} w.$$

Now, for $\mu > 0$, the *proximal operator* of μg is the map $\text{prox}_{\mu g} : \mathbb{R}^{p_2} \to \mathbb{R}^{p_2}$ defined by

$$\text{prox}_{\mu g}(v) := \arg\min_{\xi} \left\{ g(\xi) + \frac{1}{2\mu} \|\xi - v\|^2 \right\},$$

and the *Moreau envelope* $\mathcal{M}_{\mu g} : \mathbb{R}^{p_1} \to \mathbb{R}$ of μg is the optimal value associated with the above:

$$\mathcal{M}_{\mu g}(v) := g(\text{prox}_{\mu g}(v)) + \frac{1}{2\mu} \| \text{prox}_{\mu g}(v) - v \|^2.$$

Importantly for us, $\mathcal{M}_{\mu g}$ is continuously differentiable with $1/\mu$-Lipschitz gradient. In (Dhingra et al., 2019) the so-called *proximal augmented Lagrangian* associated with (3) is introduced

$$\mathcal{L}_\mu(u, \lambda) := f(u) + h(\Pi_{1u} u + \Pi_{1w} w)$$
$$+ \mathcal{M}_{\mu g}(\Pi_{2u} u + \Pi_{2w} w + \mu \lambda) - \frac{\mu}{2} \|\lambda\|^2, \tag{4}$$

which is continuously differentiable in both arguments, and the unique saddle point of which is the optimal primal-dual solution $(u^\star, \lambda^\star)$ to (3). Correspondingly, a continuous-time *proximal augmented Lagrangian method* for computing the optimal solution was given as

$$\dot{z} = \mathbb{T}(z) := \begin{bmatrix} -\nabla_u \mathcal{L}_\mu(u, \lambda) \\ \nabla_\lambda \mathcal{L}_\mu(u, \lambda) \end{bmatrix} \tag{5}$$

where $z := \text{col}(u, \lambda)$, and

$$\nabla_u \mathcal{L}_\mu(u, \lambda) = -\nabla f(u) - \Pi_{1u}^\top \nabla h(\Pi_{1u} u + \Pi_{1w} w)$$
$$- \Pi_{2u}^\top \nabla \mathcal{M}_{\mu g}(\Pi_{2u} u + \Pi_{2w} w + \mu \lambda)$$
$$\nabla_\lambda \mathcal{L}_\mu(u, \lambda) = \mu \nabla \mathcal{M}_{\mu g}(\Pi_{2u} u + \Pi_{2w} w + \mu \lambda) - \mu \lambda.$$

The following can be shown (Dhingra et al., 2019).

Proposition 2.1. If $\Pi_{2u} \Pi_{2u}^\top \succ 0$ and $\mu \geq \max\{\ell_f - \mu_f, \ell_h\}$, under Assumption 2.1, the dynamics

$$\dot{z} = \mathbb{T}(z)$$

converge exponentially to the optimal primal-dual solution $z^\star = (u^\star, \lambda^\star)$ of (3). Moreover, there exists matrix $P \succ 0$ and a constant $c > 0$ such that $W(z) := \frac{1}{2} \|z - z^\star\|_P^2$ serves as a global quadratic Lyapunov function, i.e.,

$$(z - z^\star)^\top P \, \mathbb{T}(z) \leq -c W(z), \qquad z \in \mathbb{R}^m \times \mathbb{R}^{p_2}.$$

A *feedback controller* can be obtained from (5) by replacing the steady-state output values $\bar{y}_1 = \Pi_{1u} u + \Pi_{1w} w$ and $\bar{y}_2 = \Pi_{2u} u + \Pi_{2w} w$ with the *measured* output values of $y_1(t)$ and $y_2(t)$, yielding the controller

$$\tau \dot{z} = \underbrace{\begin{bmatrix} -\nabla f(u) - \Pi_{1u}^\top \nabla h(y_1) - \Pi_{2u}^\top \nabla \mathcal{M}_{\mu g}(y_2 + \mu \lambda) \\ \mu \nabla \mathcal{M}_{\mu g}(y_2 + \mu \lambda) - \mu \lambda \end{bmatrix}}_{:= T(z,y)}. \tag{6}$$

where $\tau > 0$ is a tunable time constant. Here, note that $\mathbb{T}(z) = T(z, \Pi_u u + \Pi_w w)$. An advantage of the controller (6) is that it requires only the DC gains Π_{1u} and Π_{2u} of the plant (1) as model information. In (Colombino et al., 2020), essentially the following result is shown.

Theorem 2.2. Assume that A is Hurwitz, that Assumption 2.1 holds, $\Pi_{2u} \Pi_{2u}^\top \succ 0$ and $\mu \geq \max\{\ell_f - \mu_f, \ell_h\}$, then (i) for each $w \in \mathbb{R}^q$, the closed-loop system (1), (6) possesses a unique equilibrium point $(\bar{x}, \bar{z}^\star)$ with corresponding output $\bar{y}^\star$, and (ii) there exists $\tau^\star > 0$ such that the equilibrium point is globally exponentially stable for all $\tau > \tau^\star$.

In contrast to the underlying pure saddle flow (5), which forms the basis of the controller (6), the stability of the closed-loop system (1)–(6) is not guaranteed unconditionally. Moreover, the minimum theoretical value $\tau^\star$ required to ensure stability may be excessively large, which can significantly degrade closed-loop performance.

3. ESTIMATOR-ENHANCED FBO

Although the saddle flow (5) is unconditionally stable, the resulting closed-loop performance may be degraded because the measured output $y(t)$ deviates from its steady-state value $\bar{y} = \Pi_u \bar{u} + \Pi_w w$ during transients. Since the controller is designed to act on the steady-state output, this discrepancy limits performance. To mitigate this effect, available model information can be used to construct an estimate $\hat{\bar{y}}$ of the steady-state output and feed it into the controller (5).

3.1 Estimator Design

Since the disturbance w is constant, it is described by the simple differential equation $\dot{w} = 0$. Appending this to the model (1), we obtain the augmented system

$$\begin{bmatrix} \dot{x} \\ \dot{w} \end{bmatrix} = \underbrace{\begin{bmatrix} A & E \\ 0 & 0 \end{bmatrix}}_{:= \mathbf{A}_{\text{aug}}} \begin{bmatrix} x \\ w \end{bmatrix} + \underbrace{\begin{bmatrix} B \\ 0 \end{bmatrix}}_{:= \mathbf{B}_{\text{aug}}} u, \quad y = \underbrace{\begin{bmatrix} C_1 & 0 \\ C_2 & 0 \end{bmatrix}}_{:= \mathbf{C}_{\text{aug}}} \begin{bmatrix} x \\ w \end{bmatrix}. \tag{7}$$

To design an estimator for the augmented model (7), we require detectability of $(\mathbf{A}_{\text{aug}}, \mathbf{B}_{\text{aug}})$, which since A is Hurwitz is ensured by the following assumption.

Assumption 3.1. (**Non-Resonance**). The matrix $\begin{bmatrix} A & E \\ C_1 & 0 \\ C_2 & 0 \end{bmatrix}$ has rank $n + q$, i.e., full column rank.

Our proposed estimator-enhanced feedback-based optimization (EE-FBO) design, enhancing (6), is

$$\begin{bmatrix} \dot{\hat{x}} \\ \dot{\hat{w}} \end{bmatrix} = \mathbf{A}_{\text{aug}} \begin{bmatrix} \hat{x} \\ \hat{w} \end{bmatrix} + \mathbf{B}_{\text{aug}} u - \mathbf{L}(y - \hat{y}) \tag{8a}$$

$$\hat{y} = \mathbf{C}_{\text{aug}} \begin{bmatrix} \hat{x} \\ \hat{w} \end{bmatrix} \tag{8b}$$

$$\hat{\bar{y}} = \Pi_u u + \Pi_w \hat{w} \tag{8c}$$

$$\tau \dot{z} = T(z, y - (\hat{y} - \hat{\bar{y}})), \tag{8d}$$

where $\mathbf{L} \in \mathbb{R}^{(n+q) \times p}$ is an estimator gain to be designed and $\tau > 0$. Figure 1 shows a block diagram of the design.

The estimator generates two predictions: (i) the current output $\hat{y}$ in (8b), and (ii) the steady-state value $\hat{\bar{y}}$ in (8c) that would occur *if* u and $\hat{w}$ were constant. The estimated deviation from the steady-state is calculated as $\hat{y} - \hat{\bar{y}}$, which is subtracted from the true measurement y in the gradient control law (8d).
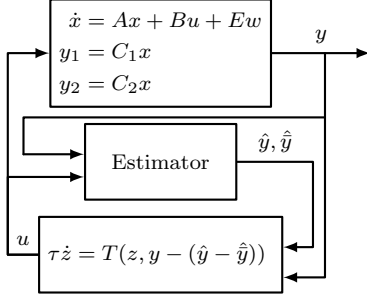
Fig. 1. Feedback-based optimization with an estimator.

3.2 Stability Analysis

We now show that incorporating the estimator ensures that the closed-loop system (1), (8) remains stable for all tunings $\tau > 0$. In other words, the time-scale separation requirement has been removed.

Theorem 3.1. Assume that A is Hurwitz, that Assumptions 2.1 and 3.1 hold, that $\Pi_{2u}\Pi_{2u}^\top \succ 0$, and that $\mu \geq \max\{\ell_f - \mu_f, \ell_h\}$. Select $\mathbf{L}$ such that $\mathbf{A}_{\text{aug}} + \mathbf{L}\mathbf{C}_{\text{aug}}$ is Hurwitz. Then (i) for each $w \in \mathbb{R}^q$, the closed-loop system (1), (8) possesses a unique equilibrium point $(x, \hat{x}, \hat{w}, z) = (\bar{x}, \bar{x}, w, \bar{z}^\star)$ with output $\bar{y}^\star$, and (ii) the equilibrium point is globally exponentially stable <u>for all</u> $\tau > 0$.

Proof of Theorem 3.1: Applying the PBH test (Hespanha, 2009, Theorem 14.2) and using Assumption 3.1, it is straightforward to show that (7) is detectable, and thus $\mathbf{L}$ can be selected such that $\mathcal{A} := \mathbf{A}_{\text{aug}} + \mathbf{L}\mathbf{C}_{\text{aug}}$ is Hurwitz. The first statement on the equilibrium follows quickly from the stability of the estimator error dynamics, the plant dynamics, and the aforementioned properties of the optimization problem (3) and saddle-point method (5). We focus therefore on stability. Define the error variables $\tilde{\zeta} := [x - \hat{x} \ \ w - \hat{w}]^\top$, and $\tilde{y} := y - \hat{y}$. In the new coordinates, the estimator dynamics (8a)–(8c) become

$$\dot{\tilde{\zeta}} = \mathcal{A}\tilde{\zeta}$$
$$\tilde{y} = \mathbf{C}_{\text{aug}}\tilde{\zeta} \qquad\qquad (9)$$
$$\dot{\hat{y}} = \Pi_u u + \Pi_w(w - \tilde{w}).$$

and the controller (8d) similarly becomes

$$\tau\dot{z} = T(z, \tilde{y} + \hat{\bar{y}})$$
$$= T(z, \Pi_u u + \Pi_w w + \tilde{v}) := F_w(z, \tilde{v}) \qquad (10)$$

where $\tilde{v} := \mathcal{C}\tilde{\zeta} = \begin{bmatrix} C & -\Pi_w \end{bmatrix}\tilde{\zeta}$. Also, note that

$$F_w(z, 0) = \mathbb{T}(z) = T(z, \Pi_u u + \Pi_w w), \qquad (11)$$

and the map $F_w(z, \tilde{v})$ is $L'_{\tilde{v}}$-Lipschitz continuous in $\tilde{v}$ where $L'_{\tilde{v}} := \max\{\|\Pi_{1u}\|\ell_h + \frac{1}{\mu}\|\Pi_{2u}\|, 1\}$ since $\nabla\mathcal{M}_{\mu g}$ is the μ^{-1}-Lipschitz continuous gradient of the convex Moreau enevelope $\mathcal{M}_{\mu g}$.

As shown in Figure 2, the closed-loop system (1), (9), (10) is a cascade, with the estimator error dynamics (9) driving the gradient flow controller (10), which in turn drives the plant (1).

Since $\mathcal{A}$ and A are both Hurwitz, global exponential stability of the (unique) equilibrium will follow (e.g., (Khalil, 2002, Lemma 4.7)) if the middle system in the cascade
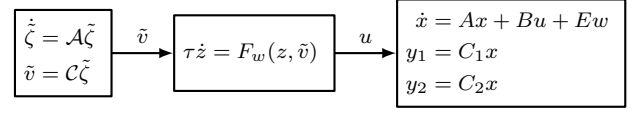

Fig. 2. Block diagram of closed-loop system in error coordinates.

is globally exponentially input-to-state stable (ISS) with respect to the equilibrium. Rewriting $F_w(z, \tilde{v})$ as

$$\dot{z} = F_w(z, 0) + \big(F_w(z, \tilde{v}) - F_w(z, 0)\big),$$

and using equation (11), we may write

$$\dot{z} = \mathbb{T}(z) + \big(F_w(z, \tilde{v}) - F_w(z, 0)\big).$$

With the ISS Lyapunov candidate $V(z) := \frac{1}{2}\|z - \bar{z}^\star\|_P^2$, we compute along trajectories that

$$\dot{V} \leq (z - \bar{z}^\star)^\top P\,\mathbb{T}(z) + \|z - \bar{z}^\star\|\|P\|\,\|F_w(z, \tilde{v}) - F_w(z, 0)\|$$
$$\leq (z - \bar{z}^\star)^\top P\,\mathbb{T}(z) + L'_{\tilde{v}}\|P\|\|z - \bar{z}^\star\|\,\|\tilde{v}\|$$
$$\leq -c\|z - \bar{z}^\star\|_P^2 + L'_{\tilde{v}}\|P\|\|z - \bar{z}^\star\|\,\|\tilde{v}\|$$

Using the Peter-Paul inequality and re-grouping, we have for any $\epsilon > 0$ that

$$\dot{V} \leq -\big(c - \frac{L'_{\tilde{v}}\|P\|}{2\lambda_{\min}(P)\epsilon}\big)\|z - \bar{z}^\star\|_P^2 + L'_{\tilde{v}}\|P\|\frac{\epsilon}{2}\|\tilde{v}\|^2.$$

Choosing $\epsilon > 0$ such that $\frac{L'_{\tilde{v}}\|P\|}{2\lambda_{\min}(P)\epsilon} < c$, we obtain the required global exponentially ISS property, which completes the proof. $\qquad\square$

4. APPLICATION TO POWER SYSTEMS

We evaluate and compare the stability and performance of the conventional FBO and EE-FBO on a power system frequency control problem with inverter-based resources (IBRs). The setup follows (Ekomwenrenren et al., 2024). The plant is a small-signal lumped mechanical frequency model of a single-area transmission system with N fast-acting dispatchable IBRs and an unknown constant power imbalance, described by

$$2H\Delta\dot{\omega} = -D\Delta\omega + \Delta P_{\text{m}} - \Delta P_{\text{u}} + \sum_{i=1}^{N}\Delta P_{\text{ibr},i} \quad (12\text{a})$$
$$T_{\text{R}}\Delta\dot{P}_{\text{m}} = -\Delta P_{\text{m}} - R_{\text{g}}^{-1}(\Delta\omega + T_{\text{R}}F_{\text{H}}\Delta\dot{\omega}) \quad (12\text{b})$$
$$\tau_i\Delta\dot{P}_{\text{ibr},i} = -\Delta P_{\text{ibr},i} + u_i, \qquad i \in \{1, \ldots, N\}, \quad (12\text{c})$$

where $\Delta\omega$ [p.u.] is the frequency deviation, ΔP_{m} [p.u.] is mechanical power change, ΔP_{u} is the unmeasured constant disturbance, $\Delta P_{\text{ibr},i}$ is the IBR power change, and u_i is the IBR power change set-point. The parameter $2H = 26.3083$ [s] is the inertia constant, $D = 0$ [p.u.] is the load damping, $T_{\text{R}} = 10$ [s] is the reheat time constant, $R_{\text{g}} = 0.05$ [p.u.] is the generator droop constant, $F_{\text{H}} = 0.64$ is the fraction of total power generated by the pressure turbine. We consider $N = 2$, with IBR time constants and $\tau_1, \tau_2 = 0.3$ [s]. Unless stated otherwise, all quantities are on the system base $S_{\text{base}} = 567.5$ MW and frequency base $f_{\text{base}} = 60$ Hz ($\omega_{\text{base}} = 2\pi f_{\text{base}}$). In this example, we formulate the optimization problem without soft constraints and time-varying cost functions as

$$\underset{u}{\text{minimize}} \quad f(u) + g(y)$$
$$\text{subject to} \quad y = \Pi_u u + \Pi_w w$$

where Π_u and Π_w are defined by (12). The control objective is to restore the frequency deviation $y = \Delta\omega$

Fig. 3. Response power system under 40MW load change under FBO and EE-FBO method.

toward zero while minimizing the IBRs output power $u = \mathrm{col}(\Delta P_{\mathrm{ibr}1}, \Delta P_{\mathrm{ibr}2})$. This is encoded through the objective functions $f(u) = \frac{1}{2}\|u\|^2$ and the *indicator function* $g(y) = \mathbb{I}_0(y)$ which has Moreau envelope $\mathcal{M}_{g\mu} = \frac{1}{2\mu}y^2$. The online optimization algorithm (8d) then becomes

$$\tau \dot{z} = \begin{bmatrix} \tau \dot{u} \\ \tau \dot{\lambda} \end{bmatrix} = \begin{bmatrix} -u - \frac{1}{\mu}\Pi_u^\top(y + \mu\lambda) \\ y \end{bmatrix} = T(z, y)$$

For the EE-FBO, the required estimator is designed using the standard linear-quadratic estimation (LQE) method, with parameters

$$Q = \mathrm{diag}(10^{-2}, 10^{-2}, 10^2, 10^2, 10^6), \qquad R = 1,$$

where the states correspond to those in (12) plus the disturbance ΔP_{u}.

We simulate the closed-loop response of the two methods over a range of tuning parameters τ, considering a load disturbance of $\Delta P_u = 40$ [MW] applied at $t = 5$ [s]. As illustrated in Figure 3a, small values of τ in the previous FBO approach results in instability and sustained oscillations. Increasing τ (Figure 3b) suppresses the oscillations but leads to slower frequency regulation and a lower (i.e., worse) frequency nadir. In contrast, EE-FBO (Figure 3c) remains stable even for small τ, yielding significantly improved transient performance. These results demonstrate that EE-FBO overcomes the inherent speed limitations of conventional FBO and enhances closed-loop performance through the use of additional model information in the form of an estimator.

5. CONCLUSION

We have introduced a method that overcomes the time-scale separation limitation of conventional FBO design. The idea is to construct a model-based estimator that predicts the system's steady-state output and incorporate this estimate into the standard FBO controller. Rigorous stability guarantees were established, and a frequency control case study demonstrated substantial performance improvements compared to conventional FBO. Future work will focus on robust and data-driven estimator constructions that reduce dependence on explicit plant models, extensions to nonlinear systems, and further applications in energy systems and robotics.

REFERENCES

Bianchin, G., Cortés, J., Poveda, J.I., and Dall'Anese, E. (2022). Time-varying optimization of LTI systems via projected primal-dual gradient flows. *IEEE Trans. Control Net. Syst.*, 9(1), 474–486. doi:10.1109/TCNS.2021.3112762.

Colombino, M., Dall'Anese, E., and Bernstein, A. (2020). Online optimization as a feedback controller: Stability and tracking. *IEEE Trans. Control Net. Syst.*, 7(1), 422–432. doi:10.1109/TCNS.2019.2906916.

Dhingra, N., Khong, S., and Jovanović, M. (2019). The proximal augmented lagrangian method for nonsmooth composite optimization. *IEEE Trans. Autom. Control*, 64(7), 2861–2868. doi:10.1109/TAC.2018.2867589.

Ekomwenrenren, E., Simpson-Porco, J.W., Farantatos, E., Patel, M., Haddadi, A., and Zhu, L. (2024). Data-driven fast frequency control using inverter-based resources. *IEEE Trans. Power Syst.*, 39(4), 5755–5768. doi:10.1109/TPWRS.2023.3337011.

Farhat, I., Ekomwenrenren, E., Simpson-Porco, J.W., Farantatos, E., Patel, M., and Haddadi, A. (2025). A multi-area architecture for real-time feedback-based optimization of distribution grids. *IEEE Trans. Smart Grid*, 16(2), 1448–1461. doi:10.1109/TSG.2024.3524622.

Hauswirth, A., He, Z., Bolognani, S., Hug, G., and Dörfler, F. (2024). Optimization algorithms as robust feedback controllers. *Annual Reviews in Control*, 57, 100941.

Hespanha, J.P. (2009). *Linear Systems Theory.* Princeton Univ Press.

Khalil, H.K. (2002). *Nonlinear Systems.* Prentice Hall, 3 edition.

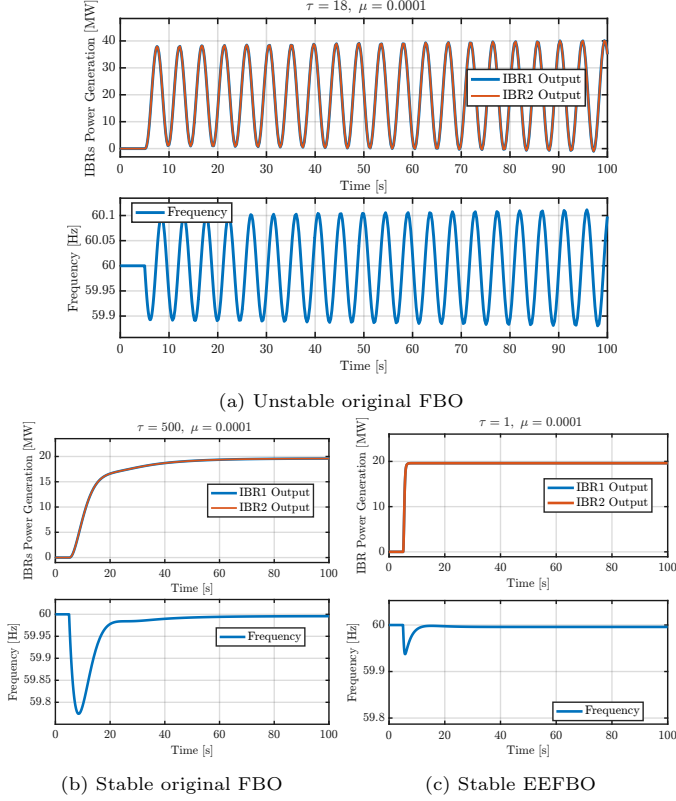Yousefi, N. and Simpson-Porco, J.W. (2025). Removing time-scale separation in feedback-based optimization via estimators. URL https://arxiv.org/abs/2511.03903.